Random spin-3/2 antiferromagnetic Heisenberg chains revisited

Yen-Tung Lin[1], **Shao-Fu Liu**[1], **Pochung Chen and**[1] **Yu-Cheng Lin**[2]
[1]Department of Physics, National Tsing Hua University, Hsinchu 300, Taiwan
[2]Graduate Institute of Applied Physics, National Chengchi University, Taipei 11605, Taiwan

Introduction

- **Extended SDRG / prior results** Extended SDRG predicts two random-singlet regimes in the bond-alternating disordered spin-$3/2$ Heisenberg chain, distinguished by $S_{\text{eff}} = 1/2$ and $S_{\text{eff}} = 3/2$, and separated by a multicritical point P_4.[Ref:1,2]
- **This work / our results** Using tSDRG, we locate P_4 from spin-correlation distributions, verify the critical exponent by finite-size scaling, and show that the VBS phase boundaries converge toward the same point.

Conclusion

- We determine the multicritical point P_4 in the disordered spin-$3/2$ Heisenberg chain. [Fig. 3]
- At weak disorder (small R), the RS critical line is less clear; introducing bond alternation enables a more reliable phase-boundary mapping that converges toward P_4. [Fig. 4]
- Remaining deviations at small R likely stem from insufficient scale separation, which limits tSDRG decimation accuracy.

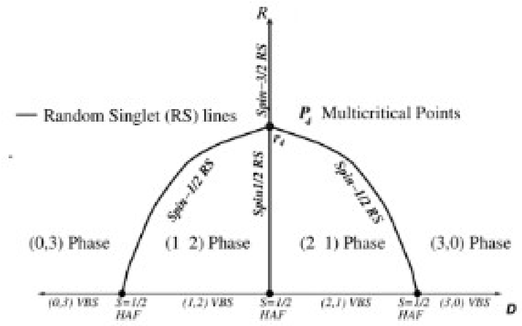

Figure 1: Schematic phase diagram for the spin-$3/2$ chain with bond alternation.

1 The Model

The Hamiltonian is given by

$$H = \sum_i J_i \, \vec{S}_i \cdot \vec{S}_{i+1}, \qquad J_i = \left(1 + D(-1)^i\right) J, \tag{1}$$

where $J_i > 0$ denotes the random antiferromagnetic coupling between neighboring sites and $\vec{S}_i$ represents the spin-$3/2$ operator at site i. The many-body properties are controlled by both the disorder strength R and the bond-alternation parameter D. In the absence of bond alternation ($D = 0$), the couplings are drawn from the power-law distribution

$$P(J) = \frac{1}{R} J^{-1+\frac{1}{R}}, \qquad 0 < J \leq 1. \tag{2}$$

2 Algorithm

Decompose the Hamiltonian into MPO blocks:

$$H = W^{[1]}W^{[2]}...W^{[L]}, W^{[i]} = \sum_{s_i, s_i^{'}} W^{s_i s_i^{'}} \left|s_i\right\rangle \left\langle s_i^{'}\right| \tag{3}$$

1. **Build a queue to store the largest gap of each pair of the local Hamiltonian:**

$$Q = \{dE_1, dE_2 ... dE_{L-1}\} \tag{4}$$

2. **Select the largest gap :** Identify the local two-site Hamiltonian with the largest energy gap dE_{max}. This pair is prioritized for coarse-graining.
3. **Build the isometric tensor:** From the diagonalization of the two-site block, construct an isometry V that selects the low-energy subspace. (the parameter χ is given to keep only the lowest χ energy eigenstates)

$$\left|\psi_k\right\rangle = \sum_{s_i, s_{i+1}} \psi_{k;s_i,s_{i+1}} \left|s_i\right\rangle \left|s_{i+1}\right\rangle, V = \sum_{k=0}^{\chi} \left|s_i\right\rangle \left|s_{i+1}\right\rangle \psi_{k;s_i,s_{i+1}} \left\langle\psi_k\right| \tag{5}$$

4. **Renormalize the MPO:** Contract the two-site MPO blocks into a single effective one-site block using the isometry V and $V^\dagger$, replacing the two-site pair with the renormalized one-site Hamiltonian.

Iterating the above four steps until the MPO train becomes a single block. This single block is treated as the effective Hamiltonian of the original Heisenberg chain.[Ref:3,4]

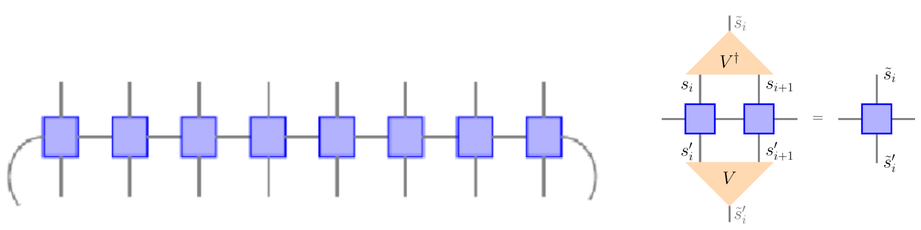

Figure 2: Left Figure: Matrix Product Operator (MPO) Structure with Periodic Boundary Conditions (PBC).[Eq:3] Right Figure: Tensor Network Representation of the Projection of the Local Hamiltonian[Eq:5]

3 Results

• End to end correlation function

The end-to-end correlation function is defined as :

$$C_1(L) = (-1)^{L-1} \left\langle\psi_{GS}\right| \vec{S_1} \cdot \vec{S_L} \left|\psi_{GS}\right\rangle \tag{6}$$

and is expected to perform a scaling collapse in the following scaling relation in P_n:

$$x = \ln C_1 / L^{\psi}, \quad \psi = \frac{1}{n} \tag{7}$$

• Multicritical point

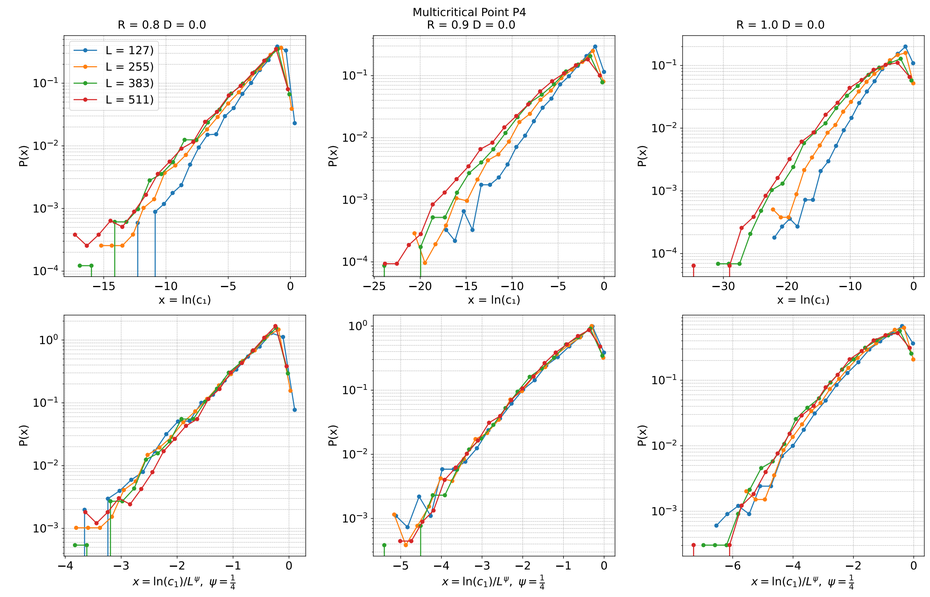

Figure 3: Distributions of the end-to-end correlation for three disorder strengths: $R = 0.8$ (left), $R = 0.9$ (middle), and $R = 1.0$ (right). Upper panels: the distribution $P(x)$ with $x = \ln c_1$ broadens as the system size L increases, a characteristic signature of the random-singlet regime. Lower panels: the same data plotted versus the scaled variable $x = \ln c_1 / L^{\psi}$ with $\psi = 1/4$, showing an improved data collapse.

• Bond Alternation: $D > 0$

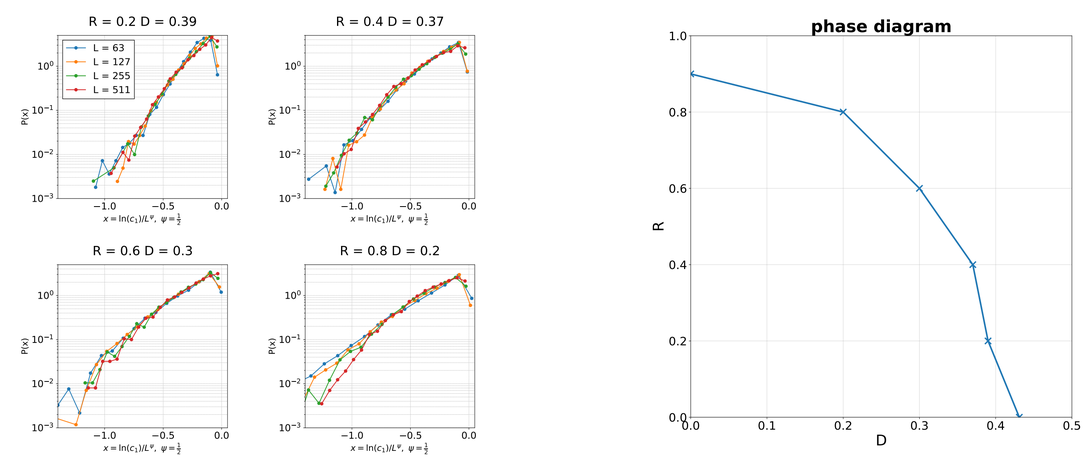

Figure 4: End-to-end correlation distributions under bond alternation for several values of R, together with the corresponding phase diagram. The quality of the P_2 scaling collapse improves systematically as R increases, indicating that the critical line evolves toward the multicritical P_4 point.

• High Disorder Region

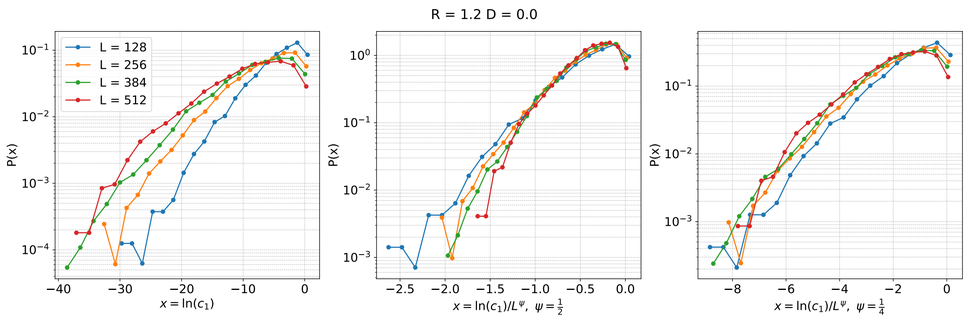

Figure 5: Distributions of the end-to-end correlation at $R = 1.2$ (and $D = 0$). Left: the distribution $P(x)$ as a function of $x = \ln c_1$ broadens with increasing system size L, consistent with random-singlet phenomenology. Middle and right: data-collapse tests using the scaled variable with $\psi = 1/2$ (random-singlet P_2 scaling) and $\psi = 1/4$ (multicritical P_4 scaling), respectively.

•Low-Disorder Region

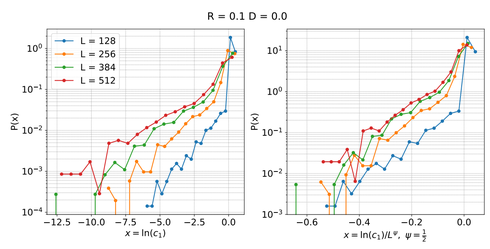

Figure 6: Distributions of the end-to-end correlation at $R = 0.1$. The distribution $P(x)$ with $x = \ln c_1$ broadens with increasing system size L. However, the collapse using the random-singlet scaling form remains imperfect, suggesting that the accessible system sizes have not yet reached the random-singlet regime.

References

1. G. Refael, S. Kehrein, and D. S. Fisher, *Spin reduction transition in spin-$3/2$ random Heisenberg chains*, Phys. Rev. B **66**, 060402(R) (2002).
2. K. Damle and D. A. Huse, *Permutation-symmetric multicritical points in random antiferromagnetic spin chains*, Phys. Rev. Lett. **89**, 277203 (2002).
3. A. M. Goldsborough and G. Evenbly, *Entanglement renormalization for disordered systems*, Phys. Rev. B **96**, 155136 (2017).
4. A. M. Goldsborough and R. A. Römer, *Self-assembling tensor networks and holography in disordered spin chains*, Phys. Rev. B **89**, 214203 (2014).